

Organic Polymorphs with Fluorescence Switching: Direct Evidences for Mechanical and Thermal Modulation of Excited State Transitions

Shan Jiang,^a Jiayu Wang,^b Qingkai Qi,^c Jingyu Qian,^a Bin Xu,^a Fangfei Li,^b Qiang Zhou,^{*b} and
Wenjing Tian^{*a}

^aState Key Laboratory of Supramolecular Structure and Materials, Jilin University, Changchun 130012, P. R. China.

^bState Key Laboratory of Superhard Materials, Jilin University, Changchun 130012, P. R. China.

^cDalian Institute of Chemical Physics, Chinese Academy of Sciences, Dalian 116023, P. R. China

*E-mail: wjtian@jlu.edu.cn; zhouqiang@jlu.edu.cn

Contents

1. Experimental Section
2. Supplementary Figures and Tables
3. References

1. Experimental Section

1.1 General Information: ^1H NMR spectra in solution were recorded on a Bruker Avance III 500-MHz spectrometer at 298 K using chloroform-d (CDCl_3) as solvent and tetramethylsilane (TMS) as the internal standard ($\delta = 0.00\text{ppm}$). ^{13}C NMR spectra were recorded on a 126 MHz BrukerAvance, using CDCl_3 as a solvent and an internal standard ($\delta = 77.00\text{ ppm}$). The GC/MS were recorded on a Thermo Fisher ITQ1100. The time of flight mass spectra was recorded using a Kratos MALDI-TOF mass system. UV-Vis spectra were recorded with a Shimadzu UV-2550 spectrophotometer. The emission spectra were measured on a Shimadzu RF-5301 PC spectrometer (CCD) and Maya2000Pro optical fiber spectrophotometer. The Φ_{F} of crystals was determined by using an integrating sphere (C-701, Labsphere Inc.). Fluorescence Lifetime and Steady State Spectroscopy were investigated using time-correlated single-photon counting (TCSPC) method and collected on an Edinburgh FLS980, with an Edinburgh EPL-375 picosecond pulsed diode laser as the excitation source. Powder X-ray diffraction data were recorded by a Rigaku 2550 diffractometer with $\text{Cu-K}\alpha$ radiation ($\lambda = 1.5418\text{ \AA}$) at 298K (scan range: $3\text{-}70^\circ$). High pressure experiments were carried out using a symmetric DAC with a pair of $500\text{ }\mu\text{m}$ culet anvils. A T301 stainless steel gasket with an initial thickness of $250\text{ }\mu\text{m}$ was preindented to $50\text{ }\mu\text{m}$ thick and a hole $120\text{ }\mu\text{m}$ in diameter was subsequently drilled in the center for the single crystal. The pressure of the sample chamber in DAC was measured by collecting ruby fluorescence spectra from ruby spheres loaded in the chamber. The pressure transmission medium (PTM), silicone oil, was also loaded in the sample chamber to

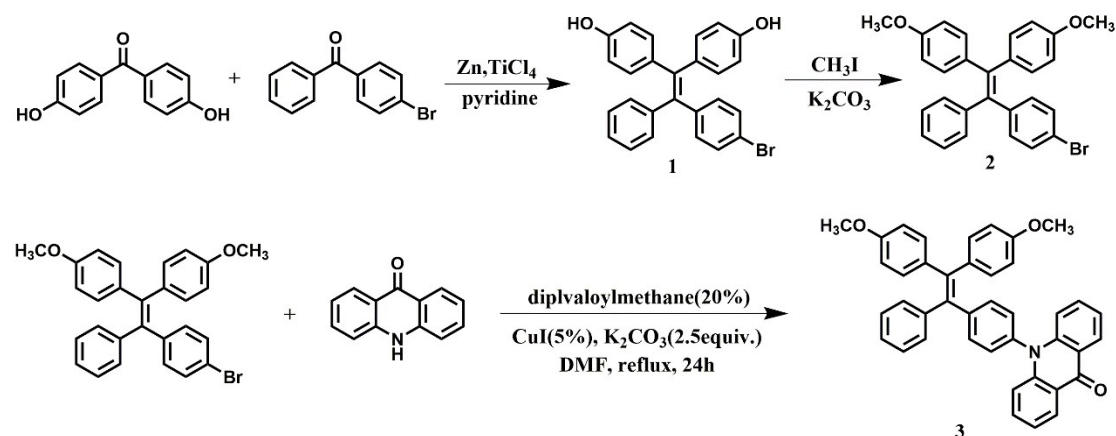
provide a hydrostatic pressure condition for the samples. PL spectroscopy measurements were conducted using a micro-Raman spectrometer (Horiba-JY) equipped with a solid-state laser ($\lambda = 325$ nm) in a backscattering configuration. The signals were dispersed by a 600 g/mm (PL) grating and collected via a 10× objective lens under high pressures, respectively. All experiments were collected at room temperature.

1.2 Single Crystal Structure Analysis: Dark C1 crystal is formed by recrystallization of the product in a mixture of ethyl acetate and petroleum ether (v/v = 1:4) and bright C2 crystal is obtained by slow crystallization of the APMOB molecule in chloroform/n-hexane solution. Single crystal X-ray diffraction intensity data were collected on a Rigaku RAXIS-PRID diffractometer using the ω -scan mode with graphite-monochromator Mo K α radiation. The structure was solved with direct methods using the SHELXTL programs and refined with full-matrix least squares on F^2 . Disordered solvent regions were treated by SQUEEZE/PLATON.¹ The crystal data can be gained for free from The Cambridge Crystallographic Data Centre via www.ccdc.cam.ac.uk/data_request/cif (CCDC: 1849786 for C1 and 1849785 for C2).

1.3 Theoretical Calculations: The DFT calculations were conducted with the Gaussian 09 series of programs using the B3LYP hybrid functional and 6-31G (d, p) basis set. The ground state structure of compound was optimized at B3LYP/6-31G (d, p) level of theory as implemented in Gaussian 09. Based on the ground state structure, its excited state structure was obtained by employing time-dependent density

functional theory within the same functional and basis sets

1.4 Synthesis



Scheme S1. Synthetic route to APMOB

Preparation of Materials: Tetrahydrofuran (THF) and ethanol were distilled in the presence of sodium benzophenone ketyl and magnesium respectively. Dimethylformamide (DMF) was distilled and dried over potassium hydroxide. All the distilled solvents were stored under nitrogen immediately prior to use. 4,4'-[2-(4-Bromophenyl)-2-phenylethenylidene]bis[phenol] (**1**) was synthesized according to previous literatures.²⁻³ All the other chemicals were purchased from Aladdin or Aldrich, and used as received without further purification.

4,4'-[2-(4-bromophenyl)-2-phenylethenylidene]bis[phenol] (**1**). ¹H NMR(500 MHz, DMSO-d₆) δ 9.38 (d, J = 21.8 Hz, 1H), 7.31 (d, J = 8.2 Hz, 1H), 7.11 (dd, J = 19.6, 7.0 Hz, 2H), 6.92 (d, J = 7.2 Hz, 1H), 6.85 (d, J = 8.0 Hz, 1H), 6.73 (t, J = 9.1 Hz, 2H), 6.50 (dd, J = 23.2, 8.1 Hz, 2H).

Synthesis of 1,1'-[2-(4-bromophenyl)-2-phenylethenylidene]bis[4-methoxybenzene] (**2**): 4,4'-[2-(4-bromophenyl)-2-phenylethenylidene]bis[phenol] (**1**) (2.14g, 4.8mmol), iodomethane (1.18ml, 19.2mmol) and potassium carbonate (3.98g, 28.8mmol) were added into acetonitrile (20mL). The mixture was stirred under reflux for 8 hours. After cooling to room temperature, the potassium carbonate was removed by vacuum filtration. The organic solvent was evaporated to give the product as the white powder (2g, 88.5%). ¹H NMR (500 MHz, Chloroform-*d*) δ 7.24 – 7.17 (m, 2H), 7.13 – 7.05 (m, 3H), 6.99 (dd, *J* = 7.7, 1.9 Hz, 2H), 6.95 – 6.86 (m, 6H), 6.68 – 6.60 (m, 4H), 3.74 (d, *J* = 13.7 Hz, 6H).

Synthesis of 1,1'-[2-(4-acridonophenyl)-2-phenylethenylidene]bis[4-methoxybenzene] (**3**): 1,1'-[2-(4-bromophenyl)-2-phenylethenylidene]bis[4-methoxybenzene] (**2**) (2g, 4.8mmol), 9(10H)-acridone (0.936g, 4.8mmol), K₂CO₃ (0.82g, 6mmol), CuI (0.14 g, 0.73mmol), 2,2,6,6-tetramethyl-3,5-heptanedione (0.3mL), and anhydrous DMF (10mL) were charged into a 50mL dry two-necked round flask. The mixture was degassed and refluxed at 152 °C under nitrogen atmosphere for 24 h. After cooling to room temperature, the precipitates from the reaction mixture were filtered and washed with 3M HCl, water and methanol. After dried in air, the obtained crude product was dissolved in CH₂Cl₂ and purified by column chromatography (silica, ethyl acetate/petroleum ether = 1/4, v/v, R_f = 0.4) to give a white powder (1.9g, 65%).⁴ ¹H NMR (500 MHz, Chloroform-*d*) δ 8.57 (dd, *J* =

8.1, 1.6 Hz, 2H), 7.53 (ddd, $J = 8.6, 6.9, 1.7$ Hz, 2H), 7.37 – 7.32 (m, 2H), 7.28 (d, $J = 1.1$ Hz, 2H), 7.24 – 7.15 (m, 5H), 7.11 – 7.06 (m, 2H), 7.06 – 6.99 (m, 4H), 6.74 (dd, $J = 9.9, 8.5$ Hz, 4H), 6.71 – 6.67 (m, 2H), 3.78 (d, $J = 7.7$ Hz, 6H). ^{13}C NMR (126 MHz, CDCl_3) δ 178.24, 158.68, 158.58, 146.35, 143.35, 143.17, 142.06, 138.17, 136.51, 136.15, 135.57, 134.02, 133.30, 132.90, 132.67, 131.37, 129.37, 128.19, 127.41, 126.73, 121.93, 121.63, 116.98, 113.29, 113.16, 55.31, 55.27. MS(EI):m/z: $[\text{M}]^+$ calcd. for $\text{C}_{41}\text{H}_{31}\text{NO}_3$:585.23; found:585.88.

2. Supplementary Figures and Tables

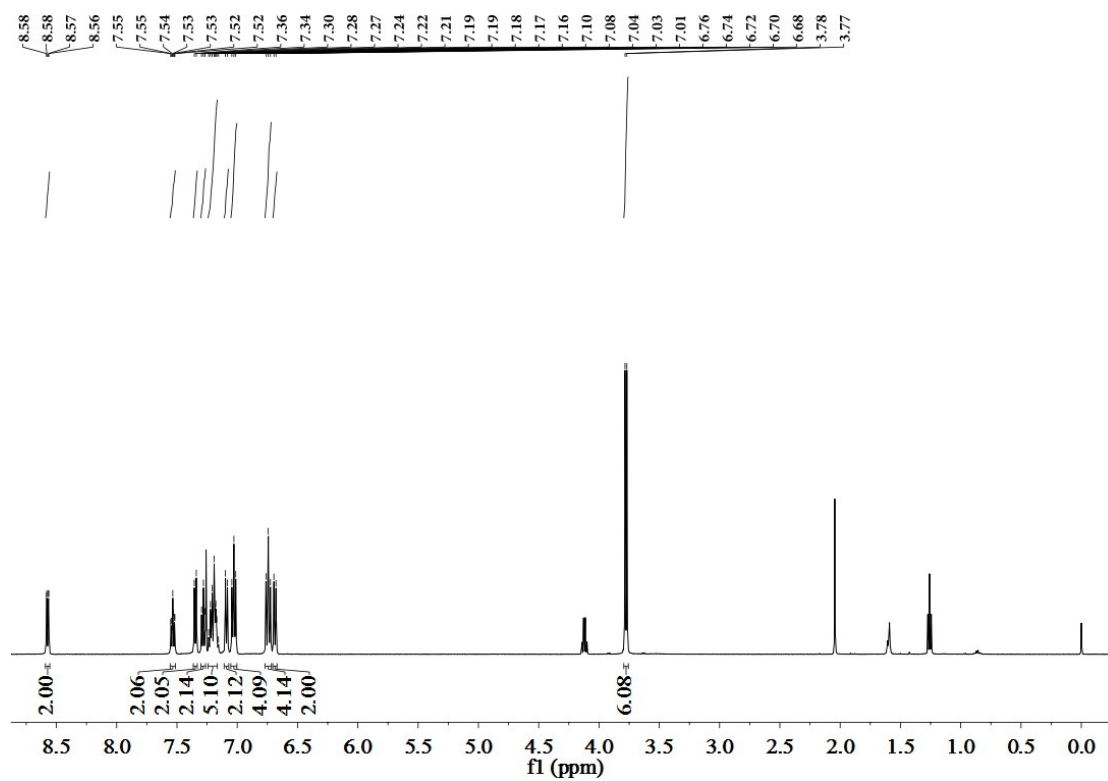


Figure S1. ¹H NMR spectrum of APMOB in CDCl₃.

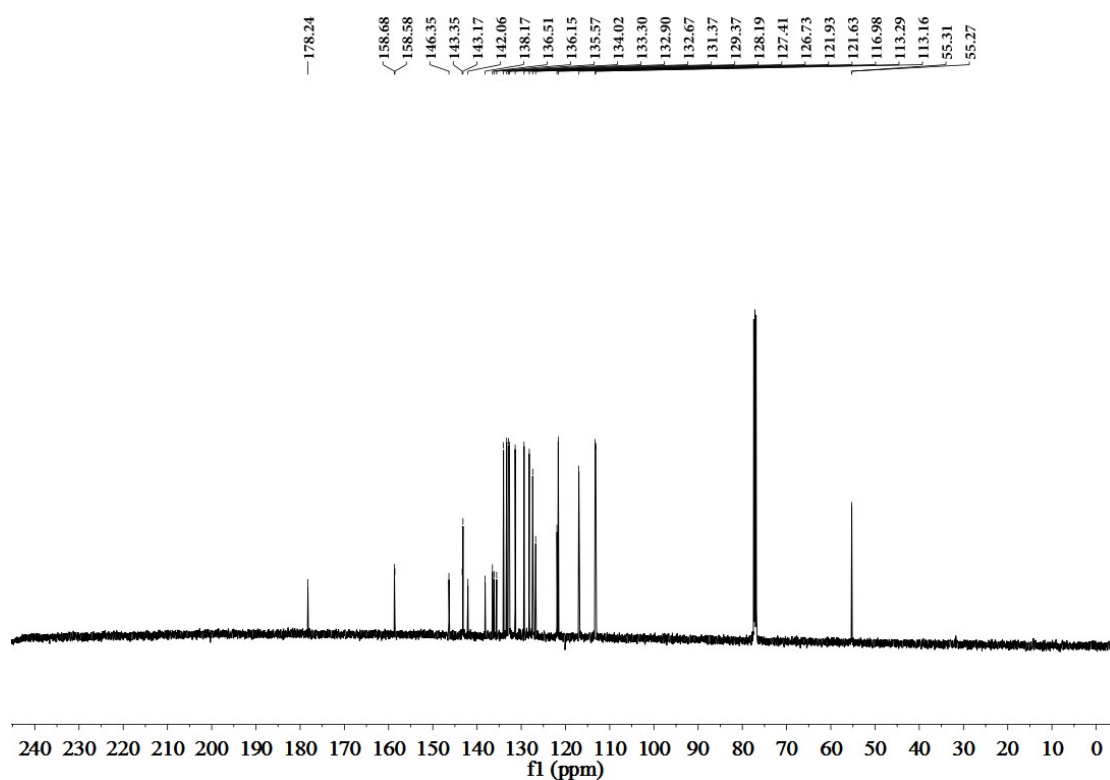


Figure S2. ¹³C NMR spectrum of APMOB in CDCl₃.

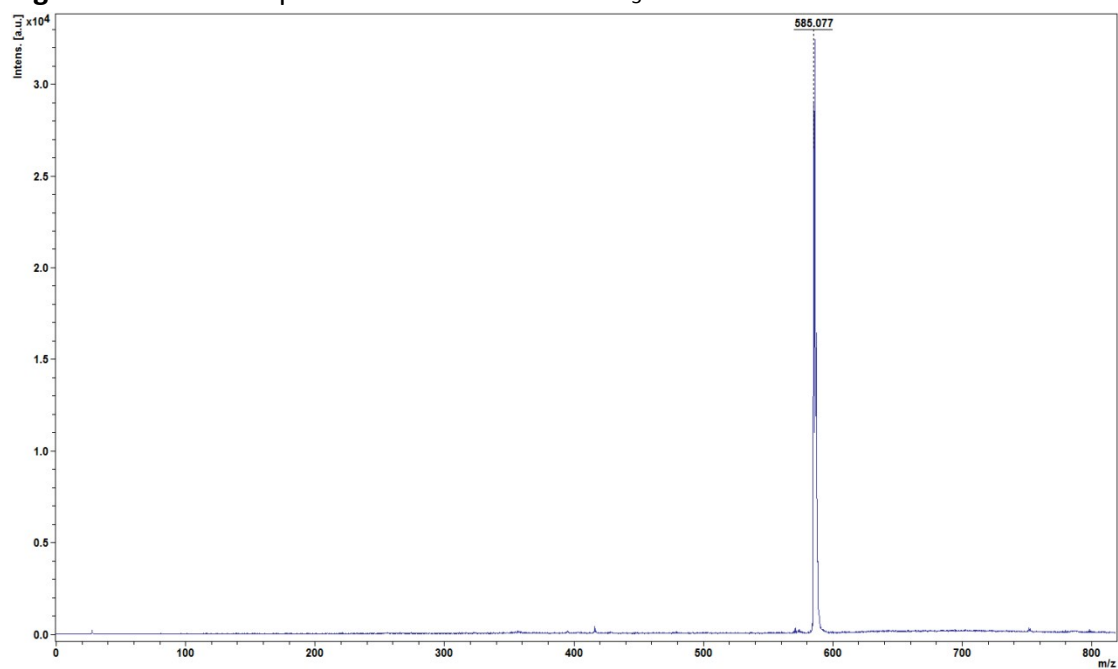


Figure S3. MS (MALDI-TOF) spectrum of APMOB.

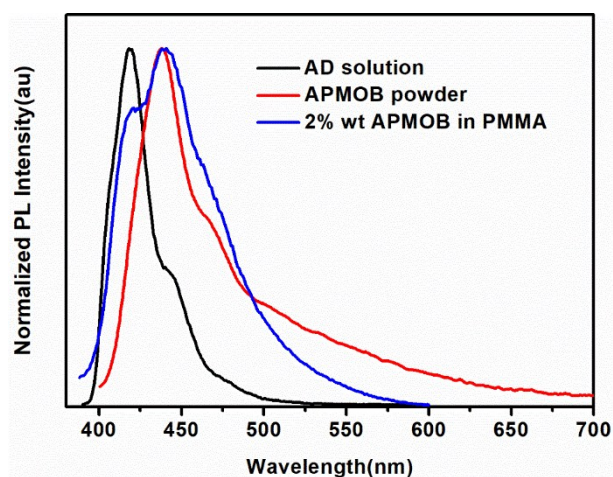


Figure S4. PL spectra of APMOB powder, PMMA film and AD in solution

Table S1. Summary of quantum yield and fluorescent lifetime of APMOB in different states.

Sample	$\Phi_F(\%)$	$\langle\tau\rangle(\text{ns})$	$K_r(\text{s}^{-1})$	$K_{nr}(\text{s}^{-1})$
C1	15	3.07	4.89×10^7	2.77×10^8
C2	60	1.46	3.97×10^8	2.88×10^8
pristine powder	7.54	1.78	4.24×10^7	5.19×10^9
ground powder	25.7	2.13	1.21×10^8	3.49×10^8
heated powder	17	1.24	1.37×10^8	6.69×10^8

Abbreviations: Φ_F : fluorescence quantum yield determined using a calibrated integrating sphere, average lifetime: $\langle\tau\rangle = (A_1\tau_1^2 + A_2\tau_2^2)/(A_1\tau_1 + A_2\tau_2)$. Radiative transition rate constant: $K_r = \Phi_F/\langle\tau\rangle$. Non-radiative transition rate constant: $K_{nr} = (1 - \Phi_F)/\langle\tau\rangle$.

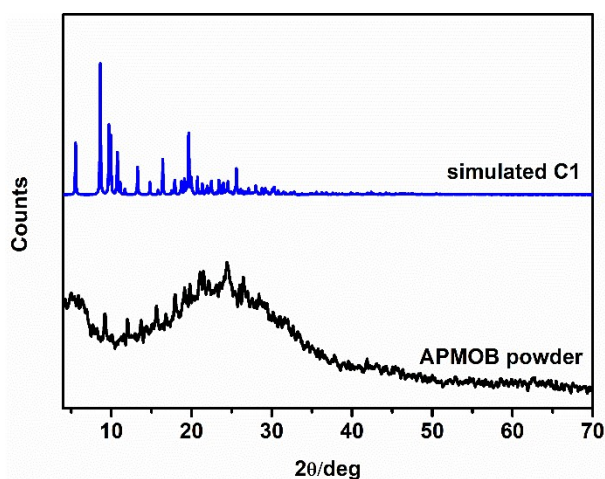


Figure S5. PXRD pattern of simulated C1 crystal and APMOB powder under different treatments.

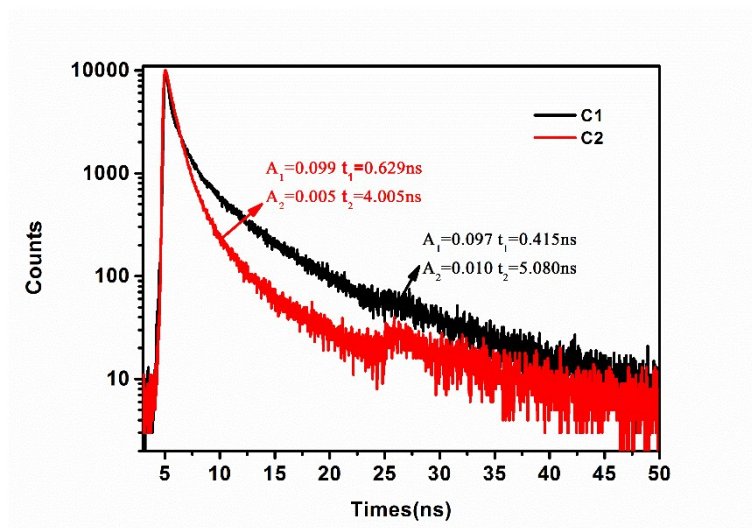


Figure S6. Lifetimes of two polymorphs measured at different emission peak.

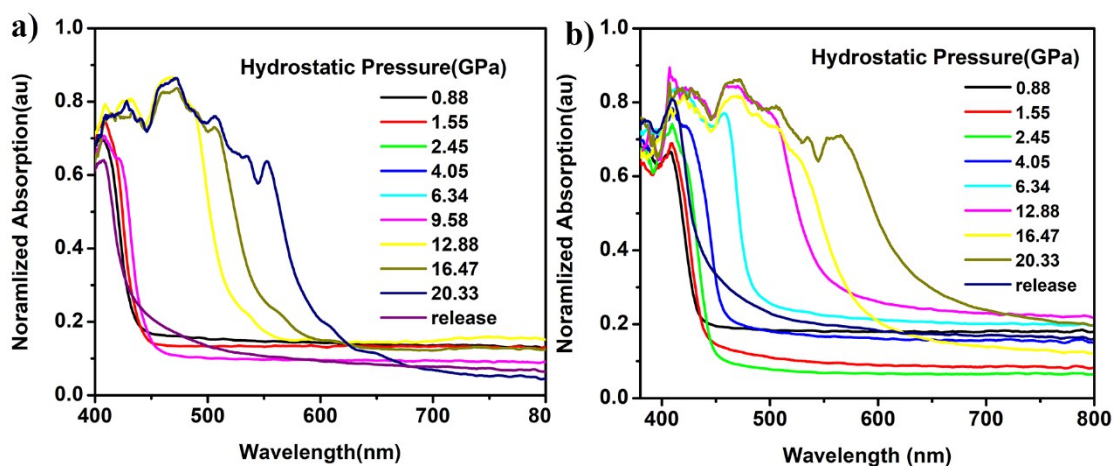


Figure S7. Absorption spectra of a) C1 and b) C2 under different hydrostatic pressure.

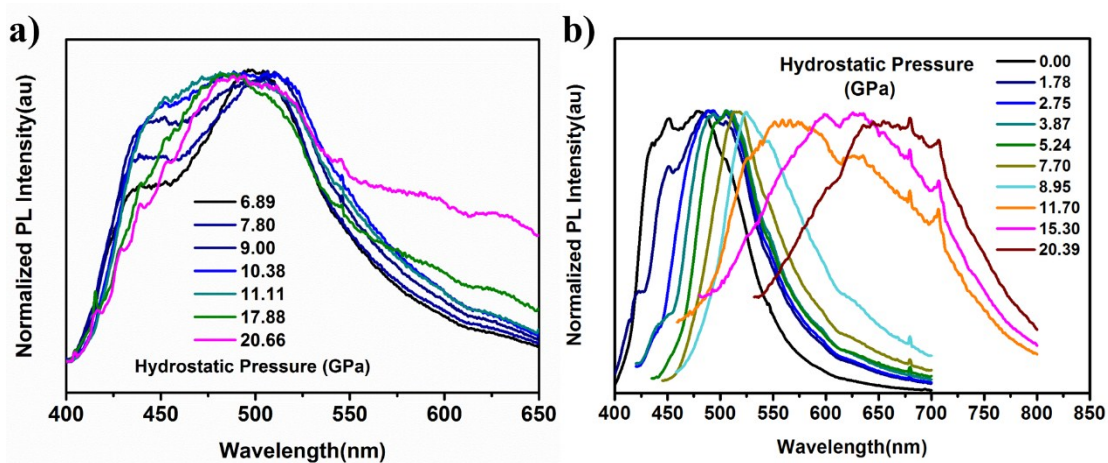


Figure S8. a-b) Fluorescence spectra of C1 (6.89-20.66GPa) and C2 (0-20.39GPa) with increasing pressure, respectively.

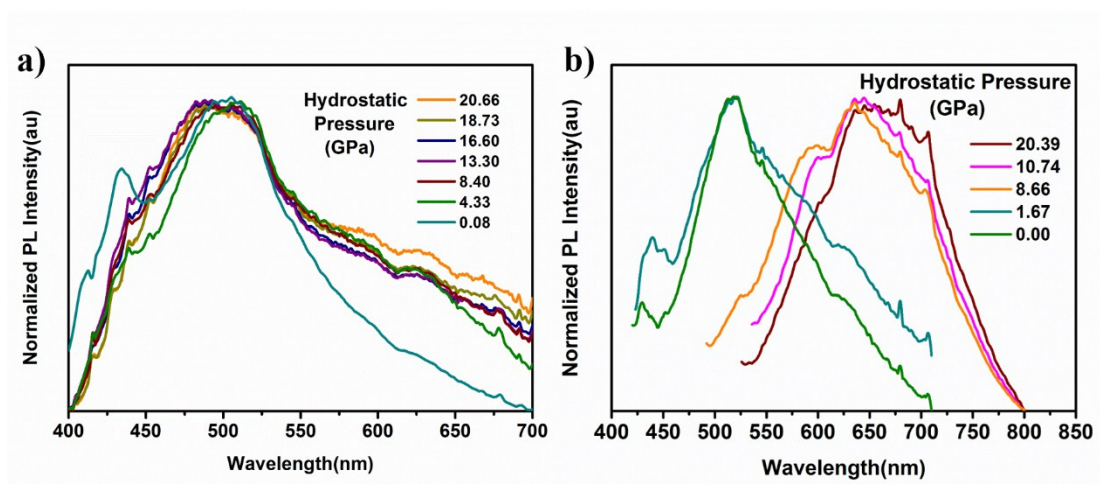


Figure S9. Fluorescence spectra of a) C1 and b) C2 under different hydrostatic pressure during decompression.

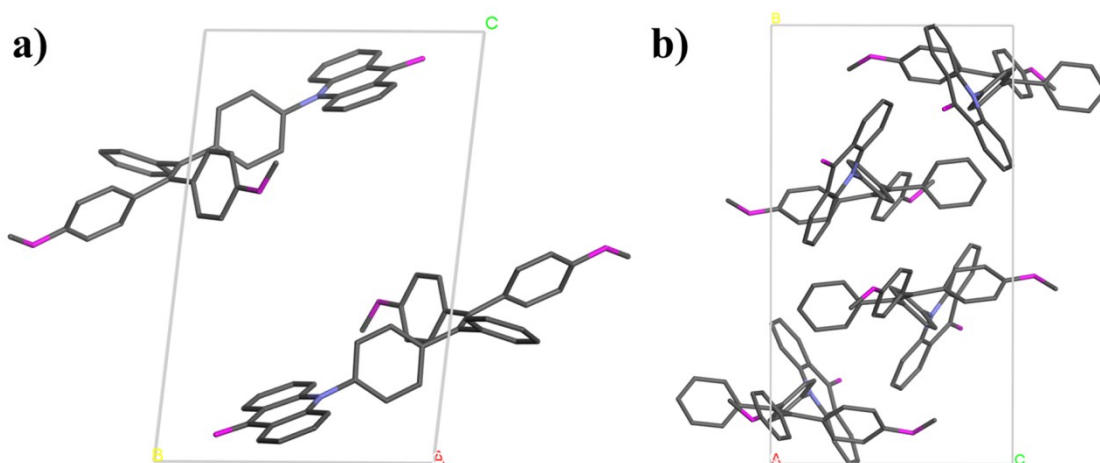


Figure S10. Crystal packing pattern of crystal a) C1 and b) C2 in one unit.

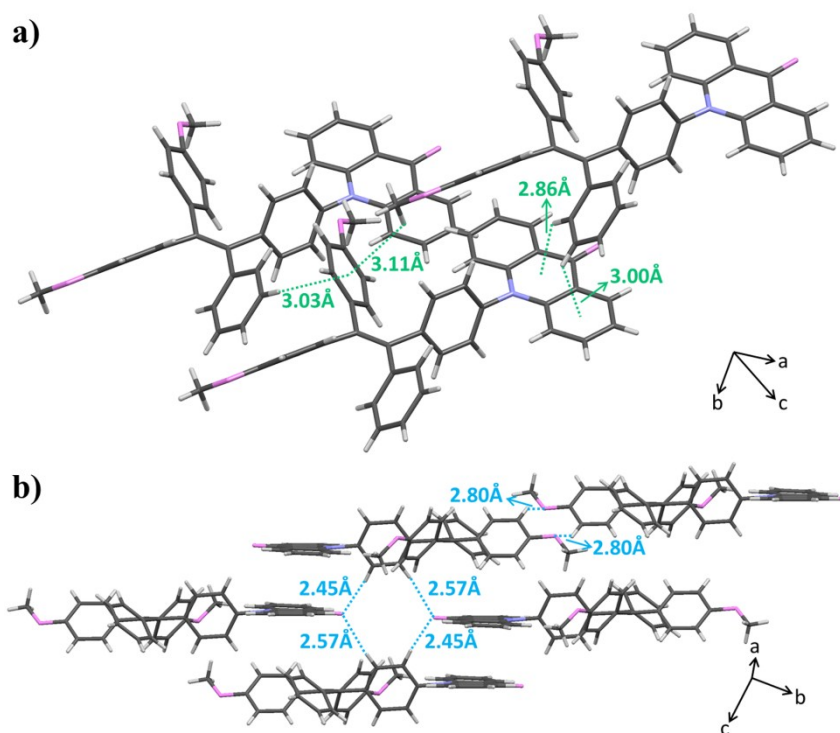


Figure S11. a) C-H... π interactions and b) C-H...O interactions in C1 crystal.

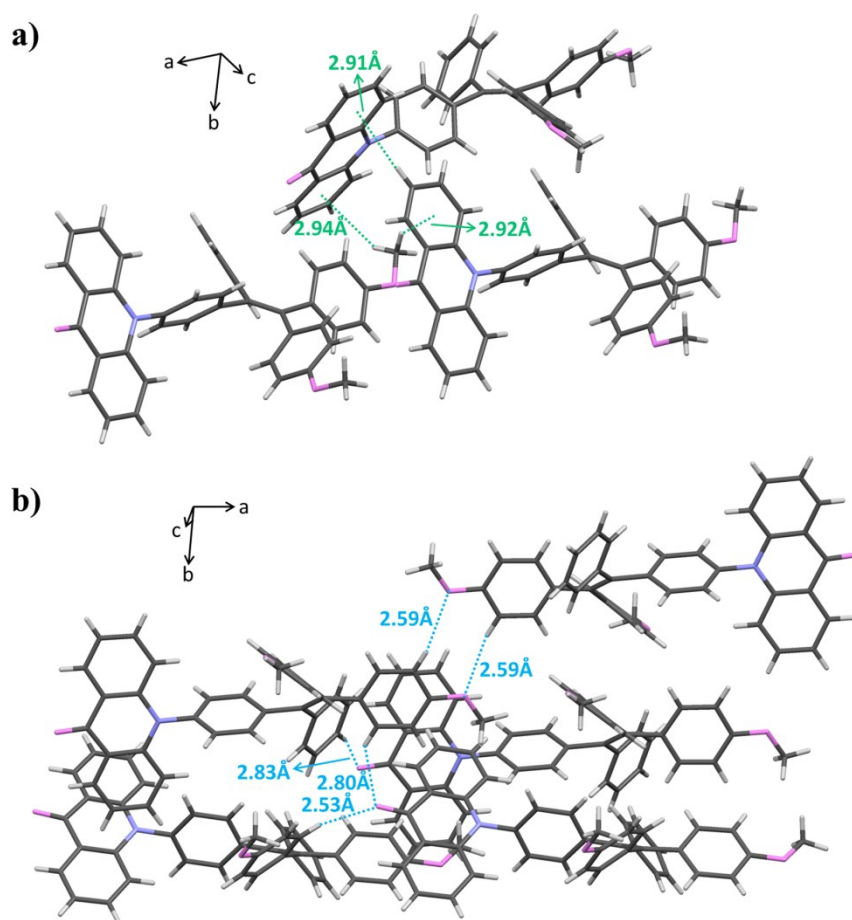


Figure S12. a) C-H... π interactions and b) C-H...O interactions in C2 crystal.

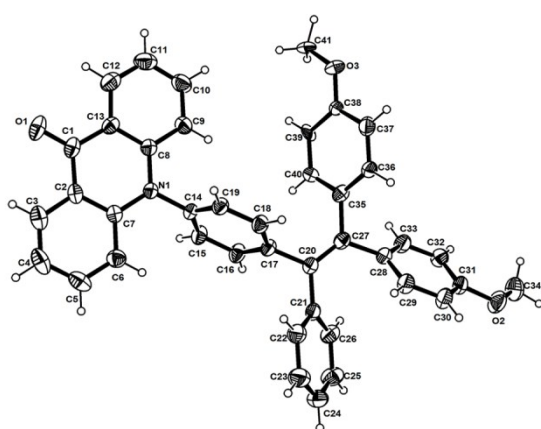
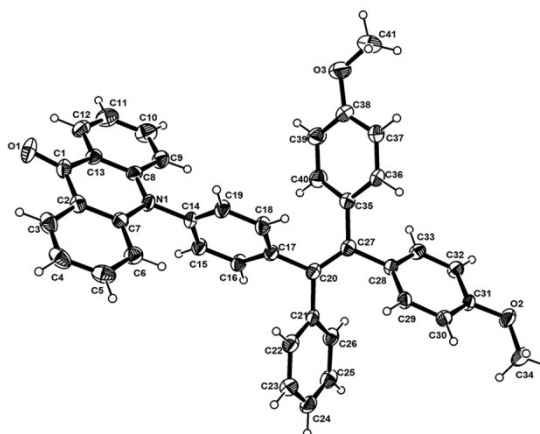
Table S2a. C-H... π interactions in two polymorphs.

Crystal	X-H...Cg	[Sym-Op]	H...Cg (Å)	X-H...Cg (°)	X...Cg (Å)
C1	C(26)-H(26)...Cg(1)	[X,-1+Y,Z]	2.86	137	3.598(1)
	C(25)-H(25)...Cg(2)	[X,-1+Y,Z]	3.00	116	3.511(1)
	C(34)-H(34A)...Cg(3)	[X,-1+Y,Z]	3.11	119	3.678(1)
	C(23)-H(23)...Cg(3)	[-1+X,Y,Z]	3.03	160	3.919(1)
C2	C(4)-H(4)...Cg(4)	[X,3/2-Y,1/2+Z]	2.91	148	3.730(3)
	C(34)-H(34C)...Cg(2)	[1+X,3/2-Y,1/2+Z]	2.94	143	3.751(3)
	C(34)-H(34A)...Cg(2)	[1+X,Y,Z]	2.92	145	3.752(3)

Footnote: Cg(1) is the centroid of N(1),C(7),C(2),C(1),C(13),C(8);
Cg(2) is the centroid of C(2),C(3),C(4),C(5),C(6),C(7);
Cg(3) is the centroid of C(35),C(36),C(37),C(38),C(39),C(40);
Cg(4) is the centroid of C(8),C(9),C(10),C(11),C(12),C(13).

Table S2b. C-H...O interactions in two polymorphs.

Crystal	Donor-H...Acceptor	[Sym-Op]	D-H (Å)	H...A (Å)	D...A (Å)	D-H...A (°)
C1	C(15)-H(15)...O(1)	[-X,1-Y,-Z]	0.93	2.45	3.362(1)	168
	C(16)-H(16)...O(1)	[X,-1+Y,Z]	0.93	2.57	3.462(1)	161
	C(30)-H(30)...O(2)	[-X,-1-Y,1-Z]	0.93	2.80	3.446(1)	127
C2	C(32)-H(32)...O(2)	[2-X,1-Y,1-Z]	0.93	2.59	3.478(3)	159
	C(24)-H(24)...O(1)	[1+X,Y,1+Z]	0.93	2.83	3.743(3)	168
	C(29)-H(29)...O(1)	[1+X,3/2-Y,1/2+Z]	0.93	2.80	3.549(3)	138
	C(36)-H(36)...O(1)	[1+X,Y,Z]	0.93	2.53	3.380(3)	152

**C1****C2**

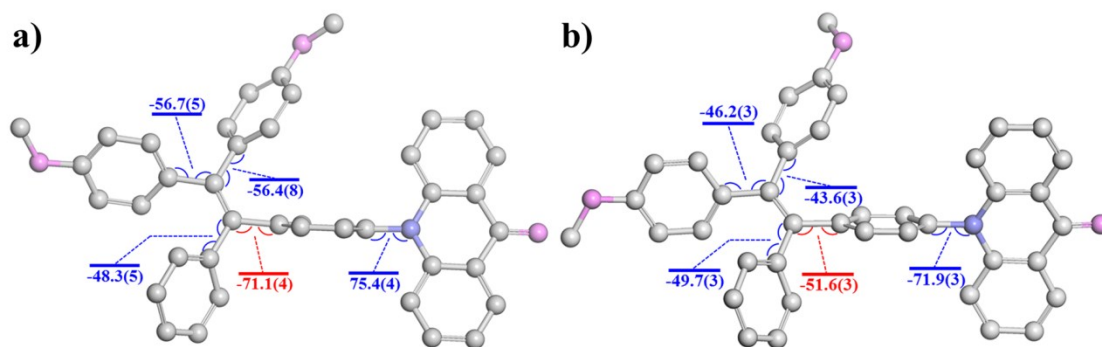


Figure S13. The torsion angle in two crystals a) C1 and b) C2 (The unit is degree).

Table S3. Summary of crystal data and intensity collection parameters of two polymorphs.

	C1	C2
Empirical formula	(C ₄₁ H ₃₁ NO ₃)·0.5(C ₄ H ₈ O ₂)·0.5(C ₅ H ₁₂)	C ₄₁ H ₃₁ NO ₃
Formula weight	665.79	585.67
Crystal dimensions, mm	0.13 × 0.12 × 0.10	0.17 × 0.14 × 0.12
Crystal system	triclinic	monoclinic
Space group	P-1	P2 ₁ /c
a, Å	10.277(2)	14.057(2)
b, Å	10.359(2)	19.813(4)
c, Å	16.047(3)	11.851(2)
α, deg	96.13(3)	90
β, deg	93.45(3)	112.567(3)
γ, deg	94.20(3)	90
V, Å ³	1690.1(6)	3047.8(9)
Z	2	4
D _{calcd.} , g/cm ³	1.308	1.276
F ₀₀₀	706	1232
Temp, (K)	293(2)	296(2)
M(Mo Kα), mm ⁻¹	0.083	0.080
θ range, deg	3.02-25.00	1.57-28.41
No. of collected reflns.	13332	22707
No. of unique reflns.	5924	7644
R(int)	0.0603	0.0809
Data/restraints/parameters	5924/0/456	7644/0/406
R1, wR2 [obs I > 2σ (I)]	0.0638, 0.1585	0.0574, 0.1027
R1, wR2 (all data)	0.1426, 0.2004	0.1711, 0.1344
Residual peak/hole e. Å ⁻³	0.26/-0.23	0.18/-0.19
Goodness-of-fit on F ²	0.897	1.003
CCDC number	1849786	1849785

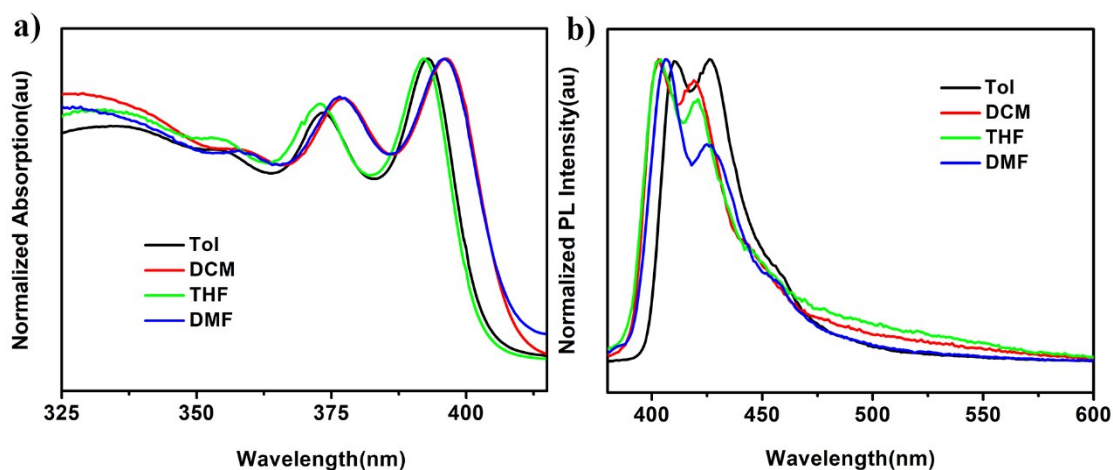


Figure S14. a) Absorption and b) PL spectra of APMOB in different solvents with increasing polarity.

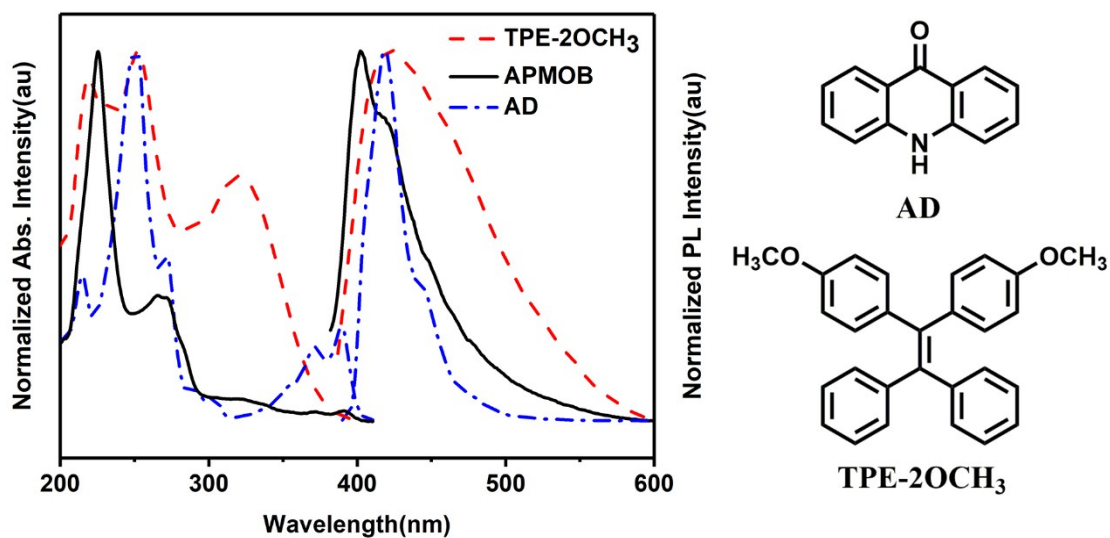


Figure S15. UV absorption and fluorescence spectra of AD, TPE-2OCH₃ and APMOB in THF solution.

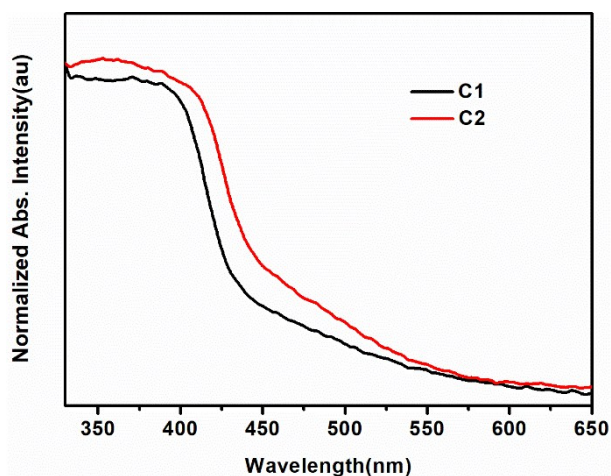


Figure S16. UV-vis absorption spectra of two polymorphs by diffuse reflectance mode.

3. References

- 1 A. L. Spek, *Acta Cryst.*, 2015, C71, 9-18
- 2 E. Zhao; Y. Chen; H. Wang; S. Chen; J. W. Lam; W. T. Leung; Y. Hong; and B. Z. Tang, *ACS Appl. Mater. Interfaces*, 2015, **7**, 7180–7188
- 3 X. F. Duan; J. Zeng; J. W. Lü; Z. B. Zhang, *Synthesis* 2007, **5**, 713–718
- 4 Q. Qi; J. Qian; X. Tan; J. Zhang; L. Wang; B. Xu; B. Zou; W. Tian, *Adv. Funct. Mater.*, 2015, **25**, 4005–4010